LEARNING FLIPPING AND ROTATION INVARIANT SPARSIFYING TRANSFORMS

Bihan Wen[1]*, Saiprasad Ravishankar* [2]*, and Yoram Bresler*[1]

[1] Department of Electrical and Computer Engineering and the Coordinated Science Laboratory
University of Illinois at Urbana-Champaign, Champaign, IL 61801, USA.
[2] Electrical Engineering and Computer Science, University of Michigan, Ann Arbor, MI 48109, USA.

ABSTRACT

Adaptive sparse representation has been heavily exploited in signal processing and computer vision. Recently, sparsifying transform learning received interest for its cheap computation and optimal updates in the alternating algorithms. In this work, we develop a methodology for learning a Flipping and Rotation Invariant Sparsifying Transform, dubbed FRIST, to better represent natural images that contain textures with various geometrical directions. The proposed alternating learning algorithm involves efficient optimal updates. We demonstrate empirical convergence behavior of the proposed learning algorithm. Preliminary experiments show the usefulness of FRIST for image sparse representation, segmentation, robust inpainting, and MRI reconstruction with promising performances.

Index Terms— Sparsifying transform, Clustering, Sparse representation, Inpainting, Magnetic resonance imaging.

1. INTRODUCTION

Sparse representation of natural signals in a certain dictionary or transform domain has been widely exploited. The popular *synthesis model* [1] suggests that a signal $y \in \mathbb{R}^n$ can be sparsely represented as $y = D\alpha + \eta$, where $D \in \mathbb{R}^{n\times m}$ is a synthesis dictionary, $\alpha \in \mathbb{R}^m$ is a sparse code, and η is a small approximation error in the signal domain. Synthesis dictionary learning methods [2] typically involve a synthesis sparse coding step which is, however, NP-hard [3]. Thus approximate solutions [4] are widely used, which are typically expensive for large-scale problems. The alternative *transform model* [5] suggests that y is approximately sparsifiable using a transform $W \in \mathbb{R}^{m\times n}$, i.e., $Wy = \alpha + e$, with $\alpha \in \mathbb{R}^m$ sparse, and e is a small approximation error in the transform domain. It is well-known that natural images are sparsifiable by analytical transforms such as discrete cosine transform (DCT), or wavelet transform. Recent works proposed learning a square sparsifying transform (SST) [6], which turns out to be advantageous in various applications such as image denoising and magnetic resonance imaging (MRI) [7–9]. Alternating minimization algorithms for learning SST have been proposed with cheap and closed-form solutions [6].

Since SST learning is restricted to one adaptive square transform for all data, the diverse patches of natural images may not be sufficiently sparsified in the SST model. Recent work focuses on learning a union of unstructured sparsifying transforms [8], dubbed OCTOBOS, to sparsify images with different contents. However, the unstructured OCTOBOS may suffer from overfitting in various applications. Hence, in this work, we propose a Flipping and Rotation Invariant Sparsifying Transform (**FRIST**) learning scheme, and show that it can provide better sparse representation by capturing the "optimal" orientations of patches in natural images.

This work was supported in part by the National Science Foundation (NSF) under grant CCF-1320953. S. Ravishankar was also supported in part by the ONR grant N00014-15-1-2141.

2. FRIST MODEL AND ITS LEARNING FORMULATION

We propose a *FRIST model* that first applies a flipping and rotation (FR) operator $\Phi \in \mathbb{R}^{n\times n}$ to a signal $y \in \mathbb{R}^n$, and models Φy as approximately sparsifiable by some sparsifying transform $W \in \mathbb{R}^{m\times n}$, i.e., $W\Phi y = x + e$, with $x \in \mathbb{R}^m$ sparse in some sense, and e small. A finite set of flipping and rotation operators $\{\Phi_k\}_{k=1}^K$ is considered, and the sparse coding problem in the FRIST model is as follows,

$$\text{(P1)} \quad \min_{1\le k\le K} \min_{z^k} \left\| W\,\Phi_k\,y - z^k \right\|_2^2 \;\; s.t. \;\; \left\| z^k \right\|_0 \le s \;\; \forall\; k$$

where the ℓ_0 "norm" counts the number of nonzeros in z^k. Thus, z^k denotes the sparse code of $\Phi_k\,y$ in the transform W domain, with maximum sparsity s. Equivalently, the optimal $\hat{z}^{\hat{k}}$ is called the optimal sparse code in the FRIST domain. We further decompose the FR matrix as $\Phi_k \triangleq G_q\,F$, where F can be either an identity matrix, or a left-to-right flipping (for 2D signals) permutation matrix. We adopt the matrix $G_q \triangleq G(\theta_q)$ which permutes the pixels in an image patch approximating rotation by angle θ_q without interpolation. Constructions of such $\{G_q\}$ have been proposed before [10, 11]. Though the number of possible permutations $\tilde{K}$ is finite, in practice we select a subset $\{\Phi_k\}_{k=1}^K$, containing a constant number $K < \tilde{K}$ of FR candidates from which the optimal $\hat{\Phi} = \Phi_{\hat{k}}$ is chosen. For each Φ_k, the optimal sparse code $\hat{z}^k$ in (P1) can be solved exactly as $\hat{z}^k = H_s(W\Phi_k y)$, where $H_s(b)$ zeros out all but the s elements of largest magnitude in $b \in \mathbb{R}^m$. The optimal $\Phi_{\hat{k}}$ is selected to provide the smallest sparsification error (objective) in (P1).

The FRIST model can be interpreted as a structured union-of-transforms model, or structured OCTOBOS [8]. In parcular, we construct each structured W_k as $W_k = W\Phi_k$, which we call a **child transform**. All of the W_k's in FRIST share a common transform W, named the **parent transform**. When the parent transform W is unitary, FRIST is also equivalent to an overcomplete synthesis dictionary model with block sparsity [12]. Compared to an overcomplete dictionary, or an OCTOBOS, FRIST is much more constrained, which turns out to be useful in inverse problems such as inpainting and MRI, preventing the overfitting of the model in the presence of limited or highly corrupted data or measurements.

Generally, the parent transform W can be overcomplete [13]. In this work, we restrict ourselves to learning FRIST with a square parent transform W, which leads to a highly efficient learning algorithm with optimal updates. Given the training data $Y \in \mathbb{R}^{n\times N}$, we formulate the FRIST learning problem as follows

$$\text{(P2)} \min_{W,\{X_i\},\{C_k\}} \sum_{k=1}^{K} \sum_{i\in C_k} \|W\Phi_k Y_i - X_i\|_2^2 + \lambda Q(W)$$
$$s.t. \;\; \|X_i\|_0 \le s \;\; \forall\; i, \;\; \{C_k\} \in \Gamma$$

where $\{X_i\}$ represent the FRIST-domain sparse codes of the corresponding columns $\{Y_i\}$ of Y. The $\{C_k\}$ indicate a clustering of the signals $\{Y_i\}$ such that each signal is associated exactly with one FR operator Φ_k. The set Γ is the set of all possible partitions of the set of integers $\{1, 2, ..., N\}$, which enforces all of the C_k's to be disjoint [8]. Problem (P2) is to minimize the FRIST learning objective that includes the modeling error $\sum_{k=1}^{K} \sum_{i \in C_k} \|W\Phi_k Y_i - X_i\|_2^2$ for Y, as well as the regularizer $Q(W) = -\log |\det W| + \|W\|_F^2$ to prevent trivial solutions [14]. Here, the penalty $-\log |\det W|$ enforces full rank on W, and $\|W\|_F^2$ helps remove 'scale ambiguity' [14] in the solution. Regularizer $Q(W)$ fully controls the condition number and scaling of the learned parent transform [14]. The regularizer weight λ is chosen as $\lambda = \lambda_0 \|Y\|_F^2$, in order to scale with the first term in (P2). Previous works [14] showed that the condition number and spectral norm of the optimal parent transform $\hat{W}$ approach 1 and $1/\sqrt{2}$ respectively, as $\lambda_0 \to \infty$ in (P2).

3. FRIST LEARNING ALGORITHM

We propose an efficient algorithm for solving (P2), alternating between *sparse coding and clustering*, and *transform update*.

Sparse Coding and Clustering. Given the training matrix Y, and fixed W, we solve (P3) for the sparse codes and clusters,

$$\text{(P3)} \quad \min_{\{C_k, X_i\}} \sum_{k=1}^{K} \sum_{i \in C_k} \|W\Phi_k Y_i - X_i\|_2^2 \quad s.t. \;\; \|X_i\|_0 \leq s \;\; \forall \; i, \;\; \{C_k\} \in \Gamma$$

The modeling error $\|W\Phi_k Y_i - X_i\|_2^2$ serves as the clustering measure corresponding to signal Y_i. Problem (P3) is to find the "optimal" FR permutation $\Phi_{\hat{k}_i}$ for each data vector that minimizes this measure. Clustering of each signal Y_i can thus be decoupled into the following optimization problem,

$$\min_{1 \leq k \leq K} \|W\Phi_k Y_i - H_s(W\Phi_k Y_i)\|_2^2 \quad \forall \; i \tag{1}$$

where the minimization over k for each Y_i determines the optimal $\Phi_{\hat{k}_i}$, or the cluster $C_{\hat{k}_i}$ to which Y_i belongs. The corresponding optimal sparse code for Y_i in (P3) is thus $\hat{X}_i = H_s(W\Phi_{\hat{k}_i} Y_i)$. Given the sparse code [1], one can also easily recover a least squares estimate of each signal as $\hat{Y}_i = \Phi_{\hat{k}_i}^T W^{-1} \hat{X}_i$. Since the Φ_k's are permutation matrices, applying and computing Φ_k^T (which is also a permutation matrix) is cheap.

Transform Update. We solve for W in (P2) with fixed $\{C_k, X_i\}$, which leads to the following problem:

$$\text{(P4)} \quad \min_{W} \left\| W\tilde{Y} - X \right\|_F^2 + \lambda Q(W)$$

where $\tilde{Y} = \left[\Phi_{\hat{k}_1} Y_1 \mid ... \mid \Phi_{\hat{k}_N} Y_N\right]$ contains signals after applying their optimal FR operations, and the columns of X are the corresponding sparse codes X_i's. Problem (P4) has a simple solution involving a singular value decomposition (SVD) [15], which is the same as the transform update step in SST [6].

Initialization and Cluster Elimination. The FRIST learning algorithm only needs initialization of the parent transform W. In Section 5.1, numerical results demonstrate the algorithm's insensitivity to parent transform initialization. To select the desired K operators, we apply a heuristic cluster elimination strategy. In the first iteration, all possible FR operators Φ_k's [10, 11] are considered for sparse coding and clustering. The learning algorithm eliminates half of the operators with smallest cluster sizes after each iteration, until the number selected drops to K. The overall computation per iteration of the proposed FRIST learning algorithm scales as $O(Kn^2N)$, which is typically lower than that of the popular overcomplete KSVD dictionary learning algorithm [16]. The full computational cost analysis, as well as convergence theory are presented elsewhere [15].

[1] The sparse code includes the value of $\hat{X}_i$, as well as the membership index $\hat{k}_i$ which adds just $\log_2 K$ bits to the code storage.

4. APPLICATIONS

FRIST learning is particularly appealing for image applications involving directional features and edges. In this section, we consider two such applications, namely robust image inpainting, and MRI.

4.1. Robust Image Inpainting

The goal of robust image inpainting is to recover missing pixels in the given image measurement, denoted as $y = \Lambda x + \varepsilon$, where $\Lambda \in \mathbb{R}^{P \times P}$ is a diagonal binary matrix with zeros only at locations corresponding to missing pixels. In robust inpainting, we consider the additive noise ε on the available pixels, since real image measurements are inevitably corrupted with noise [17]. We propose the following patch-based image inpainting formulation

$$\text{(P6)} \quad \min_{W, \{x_i, \alpha_i, C_k\}} \sum_{k=1}^{K} \sum_{i \in C_k} \left\{ \|W\Phi_k x_i - \alpha_i\|_2^2 + \tau^2 \|\alpha_i\|_0 \right\} + \sum_{i=1}^{N} \gamma \|P_i x_i - y_i\|_2^2 + \lambda Q(W)$$

Here $\{y_i\}$ and $\{x_i\}$ denote the patches extracted from x and y. The diagonal binary matrix $P_i \in \mathbb{R}^{n \times n}$ captures the available (non-missing) pixels in y_i. The sparsity penalty $\tau^2 \|\alpha_i\|_0$ is imposed, and $\gamma \|P_i x_i - y_i\|_2^2$ is the fidelity term for the ith patch, with the coefficient γ that is inversely proportional to the noise standard deviation σ. The threshold τ is proportional to σ, and also increases as more pixels are missing in y.

Our proposed iterative algorithm for solving (P6) involves the following steps: (i) sparse coding and clustering, and (ii) transform update. The sparse coding problem with sparsity penalty has closed-form solution using hard thresholding [18]. The clustering and (ii) transform update are similar to those in Section 3. Once the iterations complete, we have a (iii) patch reconstruction step, which is to solve the following problem for each patch,

$$\min_{x_i} \|W\Phi_{k_i} x_i - \alpha_i\|_2^2 + \gamma \|P_i x_i - y_i\|_2^2 \tag{2}$$

Let $\tilde{y}_i \triangleq \Phi_{k_i} y_i$, $u_i \triangleq \Phi_{k_i} x_i$, and $\tilde{P}_i \triangleq \Phi_{k_i} P_i \Phi_{k_i}^T$, where Φ_{k_i} is a permutation matrix. The rotated solution $\hat{u}_i$ in (2) is thus $\hat{u}_i = (W^T W + \gamma \tilde{P}_i)^{-1} (W^T \alpha_i + \gamma \tilde{P}_i \tilde{y}_i))$, rewritten as

$$\hat{u}_i = [B - B_{\Upsilon_i}^T (\frac{1}{\gamma} I_{q^i} + \Psi_i)^{-1} B_{\Upsilon_i}] (W^T \alpha_i + \gamma \tilde{P}_i \tilde{y}_i) \tag{3}$$

where $B \triangleq (W^T W)^{-1}$ can be pre-computed, and $\Upsilon_i \triangleq \text{supp}(\tilde{y}_i)$. Here B_{Υ_i} is the submatrix of B formed by B_{Υ_i}-indexed rows, while Ψ_i is the submatrix of B_{Υ_i} formed by B_{Υ_i}-indexed columns. The scalar $q^i = |\Upsilon_i|$ counts the number of available pixels in y_i ($q^i < n$ for inpainting). Once $\hat{u}_i$ is computed, the patch in (2) is recovered as $\hat{x}_i = \Phi_{k_i}^T \hat{u}_i$. We output the inpainted image by averaging the reconstructed patches at their respective locations. The inpainting

algorithm for (P6) is performed with multiple passes with the x_i's initialized for each pass using patches from the inpainted x in previous pass, which indirectly reinforces the dependency between overlapping patches.

4.2. MRI reconstruction

MRI image patches typically contain various oriented features [11], and have been shown to be well sparsifiable by directional wavelets [10]. The recent TL-MRI [7] scheme using adaptive SST generated superior reconstruction results. As FRIST can adapt to the MRI data, while clustering the image patches simultaneously based on their geometric orientations, we propose an MRI reconstruction method using adaptive FRIST, dubbed FRIST-MRI. For computational efficiency, we constrain the parent W to be unitary, i.e, $W^H W = I$. The FRIST-MRI problem with sparsity constraint is formulated as

$$\text{(P7)} \quad \min_{W,x,\{\alpha_i,C_k\}} \mu \left\|F_u x - y\right\|_2^2 + \sum_{k=1}^{K} \sum_{i \in C_k} \left\|W \Phi_k R_i x - \alpha_i\right\|_2^2$$
$$s.t. \ W^H W = I, \ \left\|A\right\|_0 \leq s, \ \left\|x\right\|_2 \leq L, \ \{C_k\} \in \Gamma$$

Here $x \in \mathbb{C}^P$ is the MRI image to be reconstructed, $y \in \mathbb{C}^M$ ($M \ll P$) denotes the measurements with the sensing matrix $F_u \in \mathbb{C}^{M \times P}$, which is the undersampled Fourier encoding matrix, and the operator $R_i \in \mathbb{C}^{n \times P}$ extracts overlapping patches. The constraint $\left\|x\right\|_2 \leq L$ is enforced on prior knowledge of the signal range, with some $L > 0$. The sparsity term $\left\|A\right\|_0$ counts the number of non-zeros in $A \in \mathbb{C}^{n \times P}$, whose columns are the sparse codes $\{\alpha_i\}$. This sparsity constraint enables variable sparsity levels for individual patches [7].

We use the block coordinate descent approach [7] to solve Problem (P7). The proposed algorithm alternates between (i) sparse coding and clustering, (ii) parent transform update, and (iii) MRI image reconstruction. We initialize the FRIST-MRI algorithm with the zero-filled Fourier reconstruction $F_u^H y$ for x. Step (i) solves Problem (P7) for $\{\alpha_i, C_k\}$ with fixed W and x as

$$\min_{\{\alpha_i,C_k\}} \sum_{k=1}^{K} \sum_{i \in C_k} \left\|W \Phi_k R_i x - \alpha_i\right\|_2^2$$
$$s.t. \ \left\|A\right\|_0 \leq s, \ \{C_k\} \in \Gamma \qquad (4)$$

The exact solution to (4) requires calculating the sparsification error for each possible clustering, with complexity of $O(Pn^2K^P)$, which is computationally infeasible. We instead provide an approximate solution by computing the total sparsification error (SE) for each k,

$$\sum_{i=1}^{P} SE_k^i \triangleq \min_{\{\beta_i^k\}} \sum_{i=1}^{P} \left\|W \Phi_k R_i x - \beta_i^k\right\|_2^2 \ s.t. \ \left\|B^k\right\|_0 \leq s \quad (5)$$

where the columns of B^k are $\left\{\beta_i^k\right\}$. The optimal clusters $\{C_k\}$ in 4 are approximately computed, by assigning $i \in C_{\hat{k}}$ where $\hat{k} = \arg\min_k SE_k^i$. Once the clusters are computed, the sparse codes $\hat{A}$ in (4) (for fixed clusters) is found by thresholding the matrix $\left[W \Phi_{\hat{k}_1} R_1 x \mid ... \mid W \Phi_{\hat{k}_P} R_P x\right]$ and retaining the s largest magnitude elements [7]. Step (ii) updates the parent transform W with unitary constraint. The solution, which is similar to previous work [6], involves an SVD for fixed $\{\alpha_i, C_k\}$ and x.

Step (iii) solves Problem (P7) for x, with fixed W and $\{\alpha_i, C_k\}$. It can be solved exactly using the Lagrange multiplier method [19], which is equivalent to

$$\hat{x} = \arg\min_x \sum_{k=1}^{K} \sum_{i \in C_k} \left\|W \Phi_k R_i x - \alpha_i\right\|_2^2$$
$$+ \mu \left\|F_u x - y\right\|_2^2 + \rho(\left\|x\right\|_2^2 - L) \qquad (6)$$

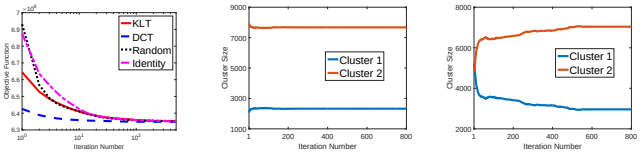

(a) FRIST Objective (b) DCT init. (c) KLT init.

Fig. 1. The plots of the convergence of (a) FRIST objective, and the cluster sizes initialized using (b) DCT, and (c) KLT.

Methods	SST	OCTOBOS	KSVD	**FRIST**
No. free parameters	64×64	128×64	64×128	64×64
USC-SIPI	34.20	33.62	35.08	**35.14**
Cameraman	29.43	29.03	30.16	**30.63**
House	36.36	35.38	37.41	**37.71**

Table 1. Reconstruction PSNR values for sparse representation using the SST, OCTOBOS, overcomplete KSVD, and FRIST methods. The best PSNR values are marked in bold.

where $\rho \geq 0$ is the optimally chosen Lagrange multiplier. It has a simple solution, and the efficient reconstruction method proposed in [7,15] can be applied, given that the parent transform W is unitary.

5. EXPERIMENTS

We present results demonstrating the promise of the FRIST framework in applications.

5.1. Convergence and Sparse Representation

We demonstrate the empirical convergence behavior, by learning a FRIST with a 64×64 parent transform W, from 10^4 randomly-extracted non-overlapping patches from the 44 images in the USC-SIPI database [20]. We set $s = 10$, $\lambda_0 = 3.1 \times 10^{-3}$, and $K = 2$ for visualization simplicity. The learning algorithm is initialized with different parent W's, including (i) Karhunen-Loève Transform (KLT), (ii) 2D DCT, (iii) random matrix with i.i.d. Gaussian entries (zero mean and standard deviation 0.2), and (iv) the identity matrix. Figure 1 illustrates the convergence of the objective function, and the cluster sizes over iterations, with different parent W initializations. The final values of the objective, and cluster sizes are identical, or similar for all the initializations. The numerical results demonstrate that our FRIST learning algorithm is reasonably robust, or insensitive to initialization. In the rest of the experiments, we initialize parent W using 2D DCT for fast convergence.

We demonstrate the usefulness of FRIST learning for image sparse representation, by re-learning the FRIST over the patches extracted from USC-SIPI with the same settings except for $K = 32$. We also train a 64×64 SST [6], 128×64 OCTOBOS [8], and 64×128 dictionary using KSVD [16] from the same training patches using $s = 10$, for comparison. With the learned models, we represent each image from the USC-SIPI database, as well as two other standard images *Cameraman* and *House* compactly by the sparse codes for their non-overlapping patches. The images are then reconstructed from their sparse representations in a least squares sense. Table 1 lists the Peak-Signal-to-Noise Ratio (PSNR) for the reconstruction. We observe that FRIST provides the best reconstruction quality compared to other adaptive sparse models, with very few trainable parameters.

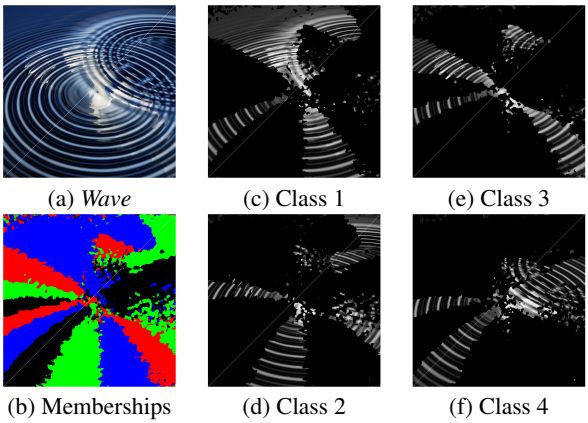

Fig. 2. Image segmentation result using FRIST learning on the gray-scale version of *Wave*. The Four different colors present the membership of pixels that belong to the four classes.

Available pixels	σ	Cubic	Smooth	DCT	SST	FRIST
20%	0	26.56	28.87	29.23	29.25	**29.33**
	5	6.40	28.64	29.21	29.24	**29.31**
	10	6.37	27.07	28.13	28.73	**29.16**
	15	6.33	25.52	26.94	28.07	**28.67**
10%	0	24.02	25.77	26.14	26.16	**26.20**
	5	5.88	25.46	25.59	25.85	**26.08**
	10	5.86	24.67	25.02	24.98	**25.46**
	15	5.82	23.73	24.19	24.47	**24.88**

Table 2. Average PSNR values for robust image inpainting of several images, using cubic interpolation (Cubic), patch smoothing (Smooth), patch-based DCT, adaptive SST, and adaptive FRIST methods. The best PSNR value in each row is marked in bold.

5.2. Image Segmentation and Clustering Behavior

The FRIST learning algorithm is capable of clustering image patches according to their orientations. We illustrate such behavior using image segmentation of the image *Wave* (512×512) shown in Fig. 2(a), which contains directional textures. We convert it into gray-scale, extract the overlapping mean-subtracted patches, learn a FRIST, and cluster the patches with $s = 10$, and $K = 4$. We aim to cluster the pixels into one of the four classes by majority voting of the overlapping patches that contain the pixel. Figure 2(b) illustrates the segmentation results, showing the pixel membership with four different colors. Figures 2(c)-(f) each visualize the image pixels clustered into a specific class in gray-scale. The results demonstrate some potential of the FRIST scheme for directional clustering. As natural images usually contain directional textures, FRIST is capable of grouping those patches with similar orientations, and thus provides better sparsification by learning directional child transforms.

5.3. Robust Image Inpainting

We present preliminary results for our adaptive FRIST-based inpainting framework. We work with a dataset of 7 standard images. We randomly remove 80% and 90% of the pixels of the entire image, and simulate i.i.d. additive Gaussian noise for the sampled pixels with $\sigma = 0$, 5, 10, and 15. We set $K = 64$, $n = 64$, and apply the proposed FRIST inpaiting algorithm to reconstruct the image. Additionally, we replace the adaptive FRIST in the inpainting algorithm with the fixed 2D DCT, and with adaptive SST [6], and compare the inpainting performance. We also compare to the cubic interpolation [21], and patch smoothing [22] methods for inpainting. Table 2 lists the image inpainting PSNR results, averaged over the seven standard images, with various amounts of sampled pixels and noise levels. The proposed adaptive FRIST inpainting scheme provides better PSNRs compared to all other inpainting methods. FRIST provides higher PSNR improvement as the noise level increases, by using a highly constrained adaptive overcomplete sparse model.

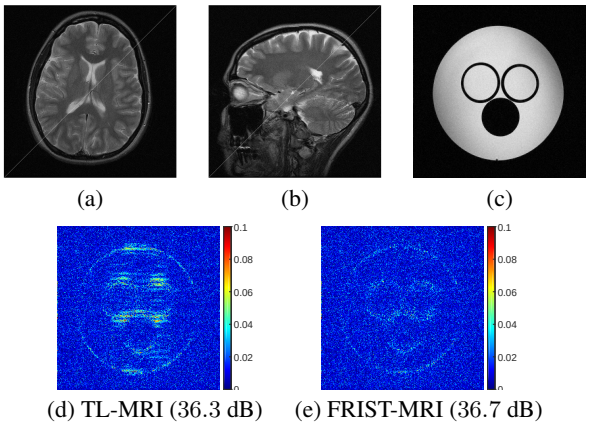

Fig. 3. Testing MRI images (a) - (c), and magnitude of reconstruction error fors image (c), using (d) TL-MRI, and (e) FRIST-MRI.

Image	Under-sampl.	Sparse MRI	DL-MRI	PANO	TL-MRI	FRIST-MRI
(a)	7× Cart.	28.6	30.9	31.1	31.2	**31.4**
(b)	5× Rand.	27.9	30.5	30.4	30.6	**30.7**
(c)	2.5× Cart.	29.9	36.6	34.8	36.3	**36.7**

Table 3. Reconstruction PSNRs using Sparse MRI, PANO, TL-MRI, and FRIST-MRI methods. The best PSNRs are marked in bold.

5.4. MRI Reconstruction

Preliminary MRI reconstruction results are presented, using the FRIST-MRI algorithm to reconstruct three complex-valued images shown in Figure 3(a)-(c) [7, 11], with various undersampling masks. We compare our results to those obtained using popular methods, including Sparse MRI [23], DL-MRI [24], PANO [25], and TL-MRI [7]. For fair comparison, we set $K = 32$, and other parameters similar to those in TL-MRI. The reconstruction PNSRs are listed in Table 3. Our proposed FRIST-MRI algorithm provides improvements over all competitors. Compared to TL-MRI, FRIST-MRI reconstruction PSNR is 0.2dB higher on average, mainly because the learned FRIST can serve as a better regularizer for MRI image reconstruction, compared to a single square transform. Figures 3(d)-3(e) visualize the magnitude of reconstruction errors, where compared to TL-MRI, FRIST-MRI generated fewer artifacts, especially along the edges of the circles.

6. CONCLUSION

We presented a method for learning a structured union-of-transforms model, dubbed FRIST, with efficient optimal updates for the block coordinate descent steps. We demonstrated the ability of FRIST learning to extract directional features in images, and it performed better than several prior methods in sparse image representation, image inpainting, and MRI reconstruction.

7. REFERENCES

[1] A. M. Bruckstein, D. L. Donoho, and M. Elad, "From sparse solutions of systems of equations to sparse modeling of signals and images," *SIAM Review*, vol. 51, no. 1, pp. 34–81, 2009.

[2] K. Engan, S.O. Aase, and J.H. Hakon-Husoy, "Method of optimal directions for frame design," in *Proc. IEEE International Conference on Acoustics, Speech, and Signal Processing*, 1999, pp. 2443–2446.

[3] G. Davis, S. Mallat, and M. Avellaneda, "Adaptive greedy approximations," *Journal of Constructive Approximation*, vol. 13, no. 1, pp. 57–98, 1997.

[4] Y. Pati, R. Rezaiifar, and P. Krishnaprasad, "Orthogonal matching pursuit : recursive function approximation with applications to wavelet decomposition," in *Asilomar Conf. on Signals, Systems and Comput.*, 1993, pp. 40–44 vol.1.

[5] W. K. Pratt, J. Kane, and H. C. Andrews, "Hadamard transform image coding," *Proc. IEEE*, vol. 57, no. 1, pp. 58–68, 1969.

[6] S. Ravishankar and Y. Bresler, "ell_0 sparsifying transform learning with efficient optimal updates and convergence guarantees," 2014, vol. 63, pp. 2389–2404.

[7] S. Ravishankar and Y. Bresler, "Efficient blind compressed sensing using sparsifying transforms with convergence guarantees and application to magnetic resonance imaging," 2015, vol. 8, pp. 2519–2557.

[8] B. Wen, S. Ravishankar, and Y. Bresler, "Structured overcomplete sparsifying transform learning with convergence guarantees and applications," *Int. J. Computer Vision*, vol. 114, no. 2, pp. 137–167, 2015.

[9] B. Wen, S. Ravishankar, and Y. Bresler, "Video denoising by online 3d sparsifying transform learning," in *IEEE International Conference on Image Processing (ICIP)*, 2015.

[10] E. L. Pennec and S. Mallat, "Bandelet image approximation and compression," *Multiscale Modeling & Simulation*, vol. 4, no. 3, pp. 992–1039, 2005.

[11] Z. Zhan, J. Cai, D. Guo, Y. Liu, Z. Chen, and X. Qu, "Fast multi-class dictionaries learning with geometrical directions in MRI reconstruction," *IEEE Trans. Biomedical Engineering*, 2015.

[12] L. Zelnik-Manor, K. Rosenblum, and Y. Eldar, "Dictionary optimization for block-sparse representations," *IEEE Transactions on Signal Processing*, vol. 60, no. 5, pp. 2386–2395, 2012.

[13] S. Ravishankar and Y. Bresler, "Learning overcomplete sparsifying transforms for signal processing," in *IEEE International Conference on Acoustics, Speech and Signal Processing (ICASSP)*, 2013, pp. 3088–3092.

[14] S. Ravishankar and Y. Bresler, "Learning sparsifying transforms," *IEEE Trans. Signal Process.*, vol. 61, no. 5, pp. 1072–1086, 2013.

[15] B. Wen, S. Ravishankar, and Y. Bresler, "FRIST - flipping and rotation invariant sparsifying transform learning and applications to inverse problems," *arXiv preprint arXiv:1511.06359*, 2016.

[16] M. Elad and M. Aharon, "Image denoising via sparse and redundant representations over learned dictionaries," *IEEE Trans. Image Process.*, vol. 15, no. 12, pp. 3736–3745, 2006.

[17] J. Mairal, M. Elad, and G. Sapiro, "Sparse representation for color image restoration," *IEEE Trans. on Image Processing*, vol. 17, no. 1, pp. 53–69, 2008.

[18] S. Ravishankar, B. Wen, and Y. Bresler, "Online sparsifying transform learning - part i: Algorithms," *IEEE Journal of Selected Topics in Signal Process.*, vol. 9, no. 4, pp. 625–636, 2015.

[19] S. Gleichman and Y. Eldar, "Blind compressed sensing," *IEEE Transactions on Information Theory*, vol. 57, no. 10, pp. 6958–6975, 2011.

[20] "The USC-SIPI Image Database," [Online: http://sipi.usc.edu/database/database.php?volume=misc; accessed July-2014].

[21] T. Yang, *Finite element structural analysis*, vol. 2, Prentice Hall, 1986.

[22] I. Ram, M. Elad, and I. Cohen, "Image processing using smooth ordering of its patches," *IEEE Transactions on Image Processing*, vol. 22, no. 7, pp. 2764–2774, 2013.

[23] M. Lustig, D. Donoho, and J. Pauly, "Sparse MRI: The application of compressed sensing for rapid mr imaging," *Magnetic resonance in medicine*, vol. 58, no. 6, pp. 1182–1195, 2007.

[24] S. Ravishankar and Y. Bresler, "MR image reconstruction from highly undersampled k-space data by dictionary learning," *IEEE Transactions on Medical Imaging*, vol. 30, no. 5, pp. 1028–1041, 2011.

[25] X. Qu, Y. Hou, F. Lam, D. Guo, J. Zhong, and Z. Chen, "Magnetic resonance image reconstruction from undersampled measurements using a patch-based nonlocal operator," *Medical image analysis*, vol. 18, no. 6, pp. 843–856, 2014.